

Generalized parton distributions of the pion in a Bethe-Salpeter approach

L. Theußl,^{*} S. Noguera,[†] and V. Vento[‡]

*Departamento de Física Teórica and Instituto de Física Corpuscular,
Universidad de Valencia-CSIC, E-46100 Burjassot (Valencia), Spain.*

(Dated: May 21, 2019)

We calculate generalized parton distribution functions in a field theoretic formalism using a covariant Bethe-Salpeter approach for the determination of the bound-state wave function. We describe the procedure in an exact calculation in scalar electrodynamics and extend the formalism to the realistic Nambu – Jona-Lasinio theory of the pion. All important features required by general physical considerations, like symmetry properties, sum rules and the polynomiality condition, are explicitly verified. We find that in the Nambu – Jona-Lasinio calculation, the generalized parton distributions do not vanish at the kinematic boundary regions, i.e. at $x = 0$ and $x = 1$, while they do in the scalar model.

PACS numbers: 24.10.Jv, 11.10.St, 13.40.Gp, 13.60.Fz

I. INTRODUCTION

Hard reactions provide important information for unveiling the structure of hadrons. The large virtuality, Q^2 , involved in these processes allows the factorization of the hard (perturbative) and soft (non-perturbative) contributions in their amplitudes. Therefore these reactions are receiving great attention by the hadronic physics community. Among the hard processes, the Deeply Virtual Compton Scattering (DVCS) merits to be singled out, because it can be expressed, in the asymptotic regime, in terms of the so called Generalized Parton Distributions (GPDs) [1, 2, 3, 4]. The GPDs describe non-forward matrix elements of light-cone operators and therefore measure the response of the internal structure of the hadrons to the probes [5, 6, 7, 8]. There is much effort under way related to the measurement of these functions.

Due to the impossibility at present to determine the GPDs from Quantum Chromodynamics directly, models have been used to provide estimates which should serve to guide future experiments [9, 10, 11, 12, 13, 14]. The aim of our work is to perform such a calculation in a field theoretic scheme which treats the bound-state wave function in a fully covariant manner following the Bethe Salpeter approach. In this way we would like to preserve all invariances of the problem. For simplicity we shall use mesons as initial and final states.

II. GENERAL FORMULAS AND KINEMATICS

The GPDs are non-diagonal matrix elements of bi-local field operators. Various conventions, reference frames, variables, etc., have been used in the literature for the description of such objects. Our notation is represented in Fig. 1, i.e., the initial momentum is labeled by P , the final momentum by P' , and the momentum transfer is given by $\Delta = P' - P$. We shall describe initially a toy model with scalar particles, the generalization to particles with spin is straightforward and will be outlined in a later section. The GPD of a scalar system is defined by the matrix elements of bi-local scalar field operators [1, 2, 3, 4]:

$$\mathcal{J}^+ \equiv \frac{1}{2} \int \frac{dz^-}{2\pi} e^{ixP^+z^-} \langle P' | \Phi^\dagger(0) \vec{\partial}^+ \Phi(z) | P \rangle \Big|_{z^+=z^-=0} = \mathcal{H}(x, \zeta, t), \quad (1)$$

where x is the conventional Bjorken variable, ζ the so-called skewedness parameter, and $\vec{\partial} = \vec{\partial} - \vec{\partial}$. The elastic electromagnetic form factor of a system composed of two scalar particles is given by:

$$J^+ \equiv \langle P' | \Phi^\dagger(0) \vec{\partial}^+ \Phi(0) | P \rangle = (P + P')^+ F(t). \quad (2)$$

^{*}Electronic address: Lukas.Theussl@uv.es

[†]Electronic address: Santiago.Noguera@uv.es

[‡]Electronic address: Vicente.Vento@uv.es

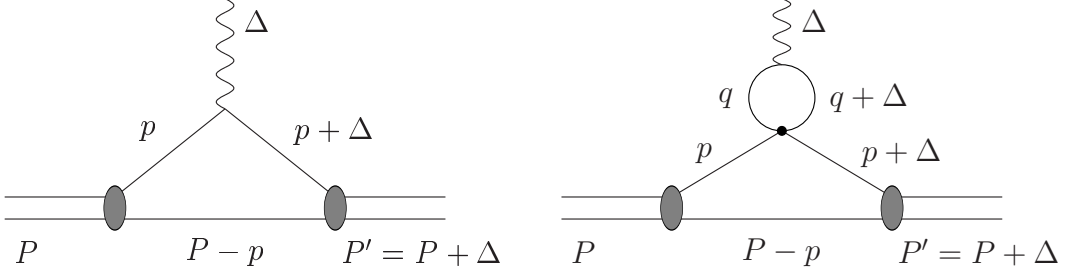


FIG. 1: Overlap diagrams up to order g for the elastic form factor.

It follows directly from these definitions that integrating the GPD over x gives the form factor,

$$\frac{2}{2-\zeta} \int \mathcal{H}(x, \zeta, t) dx = F(t), \quad (3)$$

where the dependence on the skewedness parameter ζ drops out. This result is an important constraint for any model calculation. The normalization is chosen such that $F(0) = 1$.

Let us now present our notation. Any four vector v^μ will be denoted (v^+, v^\perp, v^-) , where the light cone variables are defined by $v^\pm = (v^0 \pm v^3)/\sqrt{2}$ and the transverse part $v^\perp = (v^1, v^2)$. For the kinematics indicated in Fig. 1, we introduce the ratios

$$x = \frac{p^+}{P^+}, \quad \zeta = -\frac{\Delta^+}{P^+} \quad (4)$$

of plus-components. With this definition, both x and ζ are defined on the interval $[0, 1]$. We will only consider the distributions of one of the particles in the bound state (like the u -quark distribution in a π^+ meson), the relation of our choice of variables to other conventional definitions [15, 16] is outlined in appendix C. We are only going to consider elastic processes, so $P^2 = P'^2 = M^2$ and $\Delta^2 = t$. The following relation is true in general:

$$(\Delta^\perp + \zeta P^\perp)^2 = -\zeta^2 M^2 - (1 - \zeta)t, \quad (5)$$

the positivity of which implies an upper bound for the skewedness ζ at a given value of the momentum transfer t : $\zeta \leq (-t)/(2M^2) \left(\sqrt{1 + 4M^2/(-t)} - 1 \right) \leq 1$.

III. SCALAR ELECTRODYNAMICS

Let us start with the simplest model which allows for a completely analytic solution of the Bethe-Salpeter equation: this model describes a bound state of two equal-mass, scalar particles together with a zero-range interaction. For later convenience, we chose only one of the constituent particles to be charged. As a model Lagrangian we can then assume the one of scalar electrodynamics (SED) together with a zero-range interaction between the constituents,

$$\mathcal{L} = -\frac{1}{4}(\partial_\mu A_\nu - \partial_\nu A_\mu)^2 - \frac{\lambda}{2}(\partial \cdot A)^2 + [D_\mu \phi]^\dagger [D^\mu \phi] - m^2 \phi^\dagger \phi + \frac{1}{2} \partial_\mu \chi \partial^\mu \chi - \frac{1}{2} m^2 \chi^2 - \frac{g}{2} (\phi^\dagger \phi \chi^2), \quad (6)$$

with $D_\mu = \partial_\mu + ieA_\mu$ so that the electromagnetic charge only couples to the field ϕ . Assuming that the coupling constant g is much larger than the electromagnetic coupling constant e , we have bound states stemming from the contact interaction of the last term in Eq. (6). The corresponding Bethe-Salpeter equation is trivially solved in ladder approximation, providing the fully covariant amplitude for the bound state of total mass $M^2 = P^2$:

$$\Phi(P, p) = \frac{C}{(m^2 - p^2) (m^2 - (P - p)^2)}, \quad (7)$$

where p is the four-momentum of one of the two constituents with equal mass m , and C is a normalization constant. The spectrum for the ground state in this model is given by

$$1 = -igI(P), \quad (8)$$

where the integral $I(P)$ is given by Eq. (B2). Note that this integral is actually divergent, so some sort of renormalization would be required in order to calculate the spectrum. The theory defined by Eq. (6) is renormalizable and a renormalization program for bound states can be defined. However, for the evaluation of parton distribution functions in this model, we do not encounter any divergent integrals, we shall therefore ignore any matters of renormalization in this section. When dealing with fermionic constituents, like in the Nambu – Jona-Lasinio model discussed in the next section, we will have to specify explicitly a regularization procedure.

The model defined by the above equations is certainly not realistic enough to furnish a reasonable description of real, physical bound states, like the pion for instance. Its main advantage lies in its simplicity, the fact that one may obtain analytic solutions without approximations that violate physical requirements or symmetries, like Lorentz- or Gauge invariance, sum rules, etc. These properties make it a useful playground to perform benchmark calculations, as it was used recently in order to test the viability of certain relativistic quantum mechanics approaches [17, 18].

A. Generalized parton distribution function

An equivalent model as the one given by Eq. (6) was considered in refs. [19, 20], where the emphasis was put on the light-front quantization method. Consequently, the results are defined only for $x > \zeta$, while the region $x < \zeta$ was explored by an analytic continuation of the vertex function. However, sum rules like the one of Eq. (3) are explicitly violated in this approach.

In order to find out what happens for $x < \zeta$ we write the Generalized Parton distribution (GPD) as an integral over Bethe-Salpeter wave functions. This may be achieved with the help of Eq. (3), which provides a means for calculating the parton distribution amplitude via the integrand of the electromagnetic form factor. This procedure may be justified by the consideration of the scattering process $\gamma^* + \pi \rightarrow \gamma + \pi$, where the leading “hand-bag” diagrams reduce to the usual triangle diagram of the electromagnetic form factor in the deep inelastic limit.

Up to first order in the strong coupling constant g , we then have to calculate the two Feynman diagrams of Fig. 1 (corrections to the Bethe-Salpeter amplitude of Eq. (7) that would go beyond the ladder approximation are at least of order g^2). In scalar electrodynamics, the second diagram does not contribute to the electromagnetic form factor because of the scalar vertex function: the loop integral is proportional to

$$\int \frac{d^4 q}{(2\pi)^4} \frac{(2q + \Delta)^\mu}{(q^2 - m^2 + i\epsilon)((q + \Delta)^2 - m^2 + i\epsilon)}, \quad (9)$$

which by virtue of Eq. (B4) is zero. However, this diagram does contribute to the GPDs, because here we do not integrate over the whole four-dimensional space, but keep the $+$ -component of the integration variable fixed. But we would have to worry about regularization because the loop integral is divergent even if we do not integrate over the $+$ -component. Since we do not want to deal with regularization at this stage, and since the second diagram is of one order higher in g as compared to the first one, we will follow the conventional approach of evaluating only the first diagram¹ (impulse approximation), which leads to

$$\begin{aligned} \mathcal{H}(x, \zeta, t) &= -\frac{i}{2} \int \frac{d^2 p^\perp dp^-}{(2\pi)^4} \bar{\Phi}(P, p) (\Delta + 2p)^+ [(P - p)^2 - m^2] \Phi(P + \Delta, p + \Delta) \\ &= \frac{2x - \zeta}{2} \frac{P^+}{i} \int \frac{d^2 p^\perp dp^-}{(2\pi)^4} \bar{\Phi}(P, p) [(P - p)^2 - m^2] \Phi(P + \Delta, p + \Delta). \end{aligned} \quad (10)$$

Note that we obtain the GPD relative to a scalar probe from Eq. (10) by simply omitting the factor $2x - \zeta$. Using the Bethe-Salpeter amplitude of Eq. (7), we obtain

$$\mathcal{H}(x, \zeta, t) = \frac{2x - \zeta}{2} \frac{P^+}{i} \int \frac{d^2 p^\perp dp^-}{(2\pi)^4} \frac{C^2}{(p^2 - m^2)[(p + \Delta)^2 - m^2][(P - p)^2 - m^2]}. \quad (11)$$

Inspecting the pole structure of the integral for the evaluation of the p^- integral, we note that there is only a contribution when $0 \leq x \leq 1$, i.e., the GPDs have the correct support properties. The integral of Eq. (11) may be calculated explicitly. The analytic result for the GPD is then simply

$$\mathcal{H}(x, \zeta, t) = \frac{C^2}{16\pi^2} \frac{2x - \zeta}{2} \tilde{M}(m, \Delta, P), \quad (12)$$

¹ One can easily check, that the second diagram of Fig. 1 contributes to the GPD only in the region $0 < x < \zeta$. In view of the results that we will present, it is interesting to note that this contribution could influence the continuity of the GPDs at the crossover $x = \zeta$.

with $\tilde{M}(m, \Delta, P)$ given by Eq. (B8). Note that the momentum transfer appears in this formula only in the combination $d^\perp{}^2$, which from Eq. (5) does not depend on P^\perp , so our result is explicitly covariant. Note that the complete solution is explicitly continuous at $x = \zeta$, however, the derivative at this point is discontinuous. We furthermore encounter a zero at the point $x = \zeta/2$, which is due to the photon vertex, see Eq. (10). Had we used the variables as defined in Eq. (C1), the GPD would have no zeros as a function of x , except at the end points. The quark distribution function is given by

$$q(x) \equiv \mathcal{H}(x, 0, 0) = \frac{C^2}{4(2\pi)^2} \frac{x(1-x)}{m^2 - x(1-x)M^2}. \quad (13)$$

The normalization integral may be done analytically and gives

$$F(0) = \int_0^1 q(x) dx = \frac{C^2}{4(2\pi)^2} \frac{4m^2 \arctan \sqrt{\frac{M^2}{4m^2 - M^2}} - M^2 \sqrt{\frac{4m^2 - M^2}{M^2}}}{M^4 \sqrt{\frac{4m^2 - M^2}{M^2}}} \stackrel{!}{=} 1, \quad (14)$$

which determines the normalization constant C .

As it is not a common practice to write GPDs as integrals over Bethe-Salpeter amplitudes, we note that we can write $\mathcal{H}(x, \zeta, t)$ for $x > \zeta$ as the product of light cone wave functions [21], defined by:

$$\Psi(x, p^\perp) \equiv \frac{P^+ x(1-x)}{i\pi} \int dp^- \Phi(P, p) = -\frac{Cx(1-x)}{(p^\perp - xP^\perp)^2 + m^2 - x(1-x)M^2}, \quad (15)$$

which is non-zero only for $0 < x < 1$. Using some kinematic relations, the GPD for $x > \zeta$ may then be written as

$$\mathcal{H}(x, \zeta, t) \Big|_{x > \zeta} = \frac{1}{2} \frac{2x - \zeta}{2} \frac{(1 - \zeta)}{x(1-x)(x - \zeta)} \int \frac{d^2 p^\perp}{(2\pi)^3} \Psi^* \left(\frac{x - \zeta}{1 - \zeta}, p^\perp + \frac{1 - x}{1 - \zeta} \Delta^\perp \right) \Psi(x, p^\perp). \quad (16)$$

On the other hand, for $x < \zeta$, the GPD may not directly be written as the product of light front wave functions like in Eq. (16), even though we are still able to find analytic solutions for the integral of Eq. (11).

In Fig. 2 we give examples of GPDs in this model for different values of the binding energy and momentum transfers. We checked numerically that the sum rule of Eq. (3) is always exactly satisfied. A more stringent test is the so-called polynomiality condition [2, 3, 9], which states that the moments of the GPDs,

$$\int_0^1 dx x^{N-1} \mathcal{H}(x, \zeta, t) \equiv F_N(\zeta, t), \quad (17)$$

give functions $F_N(\zeta, t)$ that are polynomials in ζ of order not higher than N . It is difficult to verify this analytically in the general case, even with the exact solutions that we obtained. Just in the limiting case $M^2 = 0$, the following relation may be shown to hold:

$$\int_0^1 x^{N-1} \mathcal{H}(x, \zeta, 0) dx = 3 \frac{2N + (N-2) \sum_{i=1}^N \zeta^i}{N(N+1)(N+2)}, \quad (18)$$

i.e., the polynomiality condition is exactly satisfied at zero momentum transfer. Note also that for $N = 1$, Eq. (18) gives the correct normalization of Eq. (3) for any value of ζ . This shows explicitly that the sum rule is indeed independent of ζ in this case.

In the small binding limit, $M^2 \rightarrow 4m^2$, we recover the peaked nature of the GPDs, that was observed in ref. [19], where also an interpretation was given. For small binding energies, the constituents are almost free, so their wave function is highly peaked in momentum space. The two peaks at $x = 1/2$ and $x = (1 + \zeta)/2$ correspond just to the maxima of the corresponding wave function in the overlap formula Eq. (16). In the exact limit $M^2 = 4m^2$, the GPDs reduce to a sum of two δ -functions:

$$\mathcal{H}(x, \zeta, t) = \frac{1}{2} \left[\delta \left(x - \frac{1}{2} \right) + \delta \left(x - \frac{\zeta + 1}{2} \right) \right] \frac{2 - \zeta}{2} F(t), \quad (19)$$

in particular, the quark distribution function $q(x) = \mathcal{H}(x, 0, 0)$ becomes simply $q(x) = \delta(x - 1/2)$, which means that the particles are free. On the other hand, in the deep binding limit, $M^2 = 0$, and at zero momentum transfer, $t = 0$, we find the simple form

$$\mathcal{H}(x, \zeta, 0) = 6 \frac{2x - \zeta}{2} \left\{ \frac{x}{\zeta} \theta(\zeta - x) + \frac{1 - x}{1 - \zeta} \theta(x - \zeta) \right\}. \quad (20)$$

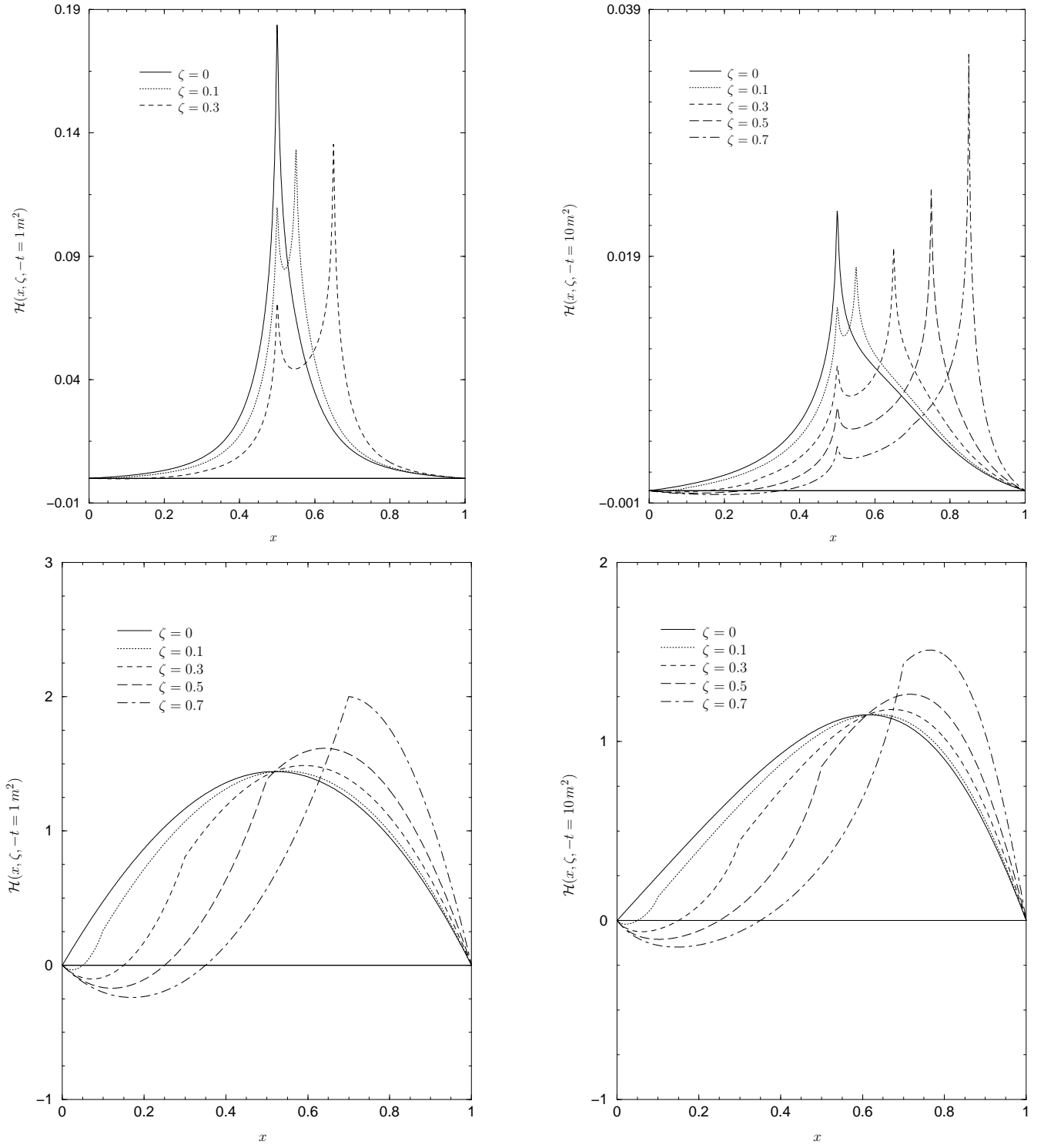


FIG. 2: Generalized parton distributions in the zero-range interaction model for different values of the bound state mass M and momentum transfers t . The top row gives results for $M/m = 2 - (1/137)^2/4$, while on the bottom $M = 0$. The graphs in the left column are for a momentum transfer $-t = 1 m^2$, and on the right, $-t = 10 m^2$. Note that the sum rule of Eq. (3) is exactly satisfied for each graph.

B. Electromagnetic form factor

Calculating the electromagnetic form factor according to Eq. (2), we find (the second diagram of Fig. 1 does not contribute as discussed above):

$$(P + P')^\mu F(Q^2) = iC^2 \int \frac{d^4 p}{(2\pi)^4} \frac{(\Delta + 2p)^\mu}{(p^2 - m^2) [(p + \Delta)^2 - m^2] [(P - p)^2 - m^2]}, \quad (21)$$

leading to

$$F(Q^2) = \frac{C^2}{16\pi^2} \int_0^1 dz \int_0^{1-z} dy \frac{1 - z - y}{m^2 + zyQ^2 - (z + y)(1 - z - y)M^2}. \quad (22)$$

The integral over y may be done analytically [18], leading to the interesting identification

$$F(Q^2) = \frac{C^2}{16\pi^2} \int_0^1 dz \frac{2}{Q} \frac{1 - z}{\sqrt{D}} \log \frac{\sqrt{D} + zQ}{\sqrt{D} - zQ} \equiv \frac{2}{2 - \zeta} \int_0^1 dx \mathcal{H}(x, \zeta, t), \quad (23)$$

with $D = 4[m^2 - z(1 - z)M^2] + z^2Q^2$. This suggests that one could calculate the GPD by a simple change of the integration variable in the expression for the form factor. The general character of this change of variable would not be clear, however. Naturally, at $Q^2 = 0$ we reproduce the normalization condition, Eq. (14).

Taking the parameters $m = 241$ MeV and $M = 139$ MeV, we can evaluate the root-mean squared radius of the pion in this model via $\langle r_\pi \rangle^2 = -6 \partial F(Q^2) / \partial Q^2 = (0.47 \text{ fm})^2$, to be compared to the experimental value of $(0.66 \text{ fm})^2$. In the limit of a mass-less bound state, $M = 0$, we obtain the analytic result $\langle r_\pi \rangle^2 = 3/(10 m^2) = (0.45 \text{ fm})^2$.

IV. THE MODEL OF NAMBU AND JONA-LASINIO

The model of the last section can certainly not provide a very realistic description of electromagnetic properties of a pion because of the scalar nature of the constituents involved. We are therefore going to consider a model with spinor particles, while for the purpose of comparison, the interaction will be as close as possible to the case considered before. An evident choice to investigate is the model of Nambu and Jona-Lasinio (NJL) [22, 23, 24, 25], which also incorporates a zero-range interaction via a four-fermion contact term. In addition, it exhibits the phenomena of dynamical mass generation and spontaneous breaking of chiral symmetry, which are crucial ingredients for low-energy hadronic physics.

The Lagrangian density in the two-flavor version of this model is given in its original form by

$$\mathcal{L} = \bar{\psi}(i\not{D} - \mu_0)\psi + g \left[(\bar{\psi}\psi)^2 - (\bar{\psi}\vec{\tau}\gamma_5\psi)^2 \right], \quad (24)$$

where we add the electromagnetic interaction in the usual way,

$$\mathcal{L} = -\frac{1}{4}(\partial_\mu A_\nu - \partial_\nu A_\mu)^2 - \frac{\lambda}{2}(\partial \cdot A)^2 + \bar{\psi}(i\not{D} - \mu_0)\psi + g \left[(\bar{\psi}\psi)^2 - (\bar{\psi}\vec{\tau}\gamma_5\psi)^2 \right], \quad (25)$$

with $D_\mu = \partial_\mu + ieA_\mu$. Again, assuming the contact interaction of the last term to be mainly responsible for the binding, the Bethe-Salpeter equation in ladder approximation to be fulfilled by a bound state in this model is given by (the factor 2 comes from the symmetry of the interaction):

$$S^{-1}(p) \Phi(P, p) S^{-1}(p - P) = ig\vec{\tau}\gamma_5 \int 2\text{Tr} \left\{ \vec{\tau}\gamma_5 \Phi(P, p') \right\} \frac{d^4 p'}{(2\pi)^4}. \quad (26)$$

Here, the symbol Tr refers to traces on spinor, flavor and color indices, and $S(p)$ is the single quark propagator

$$S(p) = \frac{i}{\not{p} - m + i\epsilon} = i \frac{\not{p} + m}{p^2 - m^2 + i\epsilon}, \quad (27)$$

of a quark with constituent mass m , which is generated from the bare mass μ_0 via the gap equation [24, 25]. The quantity $\Phi(P, p)$ is the momentum space image of the Bethe-Salpeter amplitude of a bound state with total four-momentum P , while p is the four-momentum of one of the constituents. The solution of Eq. (26) is rather trivial since the integral on the right hand side is just a constant, so we can write

$$\Phi(P, p) = igCS(p)\vec{\tau}\gamma_5 S(p - P) = -igC \frac{(\not{p} + m)\vec{\tau}\gamma_5(\not{p} - P + m)}{(p^2 - m^2)[(P - p)^2 - m^2]}, \quad (28)$$

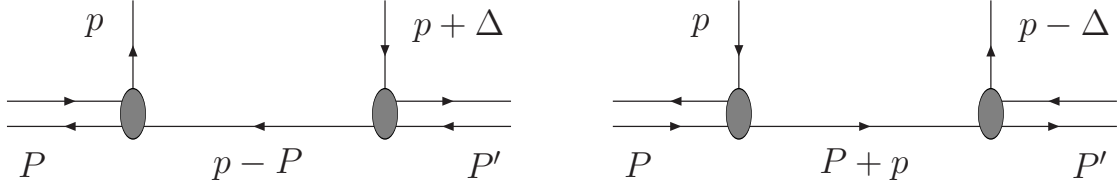


FIG. 3: Hand-Bag diagrams in the Nambu – Jona-Lasinio Model.

where C is a normalization constant. Reinserting this solution into Eq. (26) and using the definitions Eqs. (B1,B2) for the occurring integrals, gives a self-consistency condition,

$$1 = 4N_c N_f i g [2I_1 - P^2 I(P)], \quad (29)$$

which determines the mass of the ground state as a function of the coupling constant. Note that in the chiral limit, when $P^2 = 0$, Eq. (29) is nothing but the gap equation, providing some evidence for the self-consistency of the procedure.

The NJL model has been investigated quite excessively in different domains of physics with rather impressive success (see refs. [24, 25] for reviews), it is therefore natural to test its predictions for GPDs of the pion. Similar studies have been carried out recently [7, 26, 27, 28] with different models. One drawback of the NJL model is of course its non-renormalizability, which makes it useful only as an effective, low-energy model that, however, may be regarded as a non-linear realization of the QCD Lagrangian. Numerical results therefore usually depend on the regularization scheme employed to deal with the divergent integrals. As thoroughly discussed in refs. [29, 30], a suitable regularization method has to satisfy a certain number of requirements. The method that was found to be most suitable was a Pauli-Villars with two subtractions, this is the one that we shall adopt, as outlined in appendix A.

A. Generalized parton distribution

We are interested in calculating the hand-bag diagrams of Fig. 3 in the Nambu – Jona-Lasinio Model. A general expression for the matrix element of the bi-local fermionic current in the Bethe-Salpeter approach is

$$\begin{aligned} \langle P' | \bar{\Psi}(x') \gamma_\mu \Psi(x) | P \rangle &= \int d^4 x_2 \text{Tr} \left\{ \bar{\Phi}_{P'}(x', x_2) \gamma_\mu [\Phi_P(x, x_2) (i\vec{\partial}^{(2)} - m_2)] \right\} \\ &+ \int d^4 x_1 \text{Tr} \left\{ \bar{\Phi}_{P'}(x_1, x) (i\vec{\partial}^{(1)} - m_1) \Phi_P(x_1, x') \gamma_\mu \right\}, \end{aligned} \quad (30)$$

where the first (second) term in this expression corresponds to the contribution of the first (second) constituent of the system, and indices 1 and 2 refer to coordinates or operators related to particles 1 and 2 bound in the meson. In terms of momentum variables we have

$$\Phi_P(x_1, x_2) = e^{-iP \cdot X} \int \frac{d^4 k}{(2\pi)^4} e^{-ikr} \Phi(k, P), \quad (31)$$

with the center-of-mass and relative coordinates defined by

$$X = \mu_1 x_1 + \mu_2 x_2, \quad r = x_1 - x_2, \quad \mu_{1,2} = \frac{m_{1,2}}{m_1 + m_2}, \quad (32)$$

and $P = p_1 + p_2$, $k = \mu_2 p_1 - \mu_1 p_2$ the total and relative four-momentum of the system. We shall concentrate on the u -quark parton distribution in a π^+ meson, for which we have to consider the first diagram of Fig. 3, with $p_1 = p$, $p_2 = P - p$. The second diagram of Fig. 3 would correspond to the d -quark parton distribution with $p_1 = -p$, $p_2 = P + p$. Inserting Eq. (31) and taking $m_1 = m_2 = m$, we have for the hand-bag contribution to the GPD:

$$\begin{aligned} \frac{1}{2} \int \frac{dz^-}{2\pi} e^{ixP^+ z^-} \langle P' | \bar{\Psi}(0) \gamma^+ \Psi(z) | P \rangle \Big|_{z^+ = z^\perp = 0} &= \mathcal{H}(x, \zeta, t) = \\ &= \frac{1}{2} \int \frac{d^4 p}{(2\pi)^4} \delta(x - p^+ / P^+) \text{Tr} \left\{ \bar{\Phi}(p + P' - P, P') \gamma^+ \Phi(p, P) (\not{p} - \not{P} - m) \right\}, \end{aligned} \quad (33)$$

where we have switched back to particle momenta. With the adjoint of the Bethe-Salpeter amplitude

$$\bar{\Phi}(P, p) = \gamma_0 \Phi^\dagger(P, p) \gamma_0 = igC^* \frac{[(\not{p} - \not{P} + m)\vec{\tau}\gamma_5(\not{p} + m)]}{(p^2 - m^2)[(P - p)^2 - m^2]}, \quad (34)$$

we perform the integral over p^+ , and using Eqs. (28,34), we obtain an expression for the GPD in the Nambu – Jona-Lasinio model that is similar to Eq. (11):

$$\mathcal{H}(x, \zeta, t) = \frac{4N_c N_f}{2} ig^2 C^2 \int \frac{d^2 p^\perp P^+ dp^-}{(2\pi)^4} \frac{(x+1-\zeta)(p^2 - m^2) + p \cdot \Delta - xP \cdot \Delta - (2x-\zeta)p \cdot P}{(p^2 - m^2)[(p+\Delta)^2 - m^2][(P-p)^2 - m^2]}. \quad (35)$$

The p^- integral in Eq. (35) is evaluated by the usual residue calculus. Due to the pole structure of the integrand we obtain two contributions, the first one in the region $\zeta < x < 1$, corresponding to the quark contribution and the second in the region $0 < x < \zeta$, corresponding to a quark-anti-quark contribution. The second diagram of Fig. 3 will give an anti-quark contribution in the region $\zeta - 1 < x < 0$, and a sea-quark contribution in the region $0 < x < \zeta$, just like the first diagram. In case of a π^+ meson, the first diagram gives the u -quark distribution, while the second one gives the \bar{d} -quark distribution, but due to iso-spin symmetry, both distributions are related by $\mathcal{H}_u(x, \zeta, t) = -\mathcal{H}_{\bar{d}}(\zeta - x, \zeta, t)$. Concentrating only on the u -quark distribution, we find for $x > \zeta$:

$$\mathcal{H}(x, \zeta, t) \Big|_{x>\zeta} = \frac{N_c N_f g^2 C^2}{2} \int \frac{d^2 p^\perp}{(2\pi)^3} \left\{ \frac{1}{p^{\perp 2} + m^2 - \bar{x}M^2} + \frac{1}{(p^\perp + d^\perp)^2 + m^2 - \bar{y}M^2} \right. \\ \left. + \frac{y[(2x-\zeta)M^2 + (1-x)t]}{[p^{\perp 2} + m^2 - \bar{x}M^2][(p^\perp + d^\perp)^2 + m^2 - \bar{y}M^2]} \right\}, \quad (36)$$

with the abbreviations $\bar{x} = x(1-x)$, $\bar{y} = y(1-y)$, $y = (1-x)/(1-\zeta)$ and $d^\perp = y(\Delta^\perp + \zeta P^\perp)$.

With the Pauli-Villars regularization method, the final integrals in Eq. (36) may readily be evaluated, so we get the analytic expression for the GPD in the Nambu – Jona-Lasinio model for $x > \zeta$:

$$\mathcal{H}(x, \zeta, t) \Big|_{x>\zeta} = \frac{N_c N_f g^2 C^2}{2} \frac{1}{(2\pi)^2} \sum_{j=0}^2 c_j \left\{ -\log \frac{m_j^2}{m^2} - \frac{1}{2} \log \frac{m_j^2 - \bar{x}M^2}{m_j^2} - \frac{1}{2} \log \frac{m_j^2 - \bar{y}M^2}{m_j^2} \right. \\ \left. + \frac{(2x-\zeta)M^2 + (1-x)t}{2} \tilde{M}(m_j, \Delta, P) \right\}, \quad (37)$$

with $\tilde{M}(m, \Delta, P)$ given by Eq. (B8) and $m = m_0$. We note that the first three terms in the curly bracket of Eq. (37), which stem from the divergent first two integrals in Eq. (36), give contributions that are independent of the momentum transfer t . The first term, in particular, gives an overall constant, independent of x , ζ and t , which does not vanish for $x = 1$. From Eq. (37) one can determine the normal distribution function at zero momentum transfer,

$$q(x) = \mathcal{H}(x, 0, 0) = \frac{N_c N_f g^2 C^2}{2(2\pi)^2} \sum_{j=0}^2 c_j \left\{ -\log \frac{m_j^2}{m^2} - \log \frac{m_j^2 - \bar{x}M^2}{m_j^2} + \frac{m_j^2}{m_j^2 - \bar{x}M^2} \right\}, \quad (38)$$

from which we get the normalization condition

$$\int_0^1 \mathcal{H}(x, 0, 0) dx = \frac{N_c N_f g^2 C^2}{2(2\pi)^2} \sum_{j=0}^2 c_j \left\{ -\log \frac{m_j^2}{m^2} + \frac{2(M^2 - 2m_j^2)}{M\sqrt{4m_j^2 - M^2}} \arctan \frac{M}{\sqrt{4m_j^2 - M^2}} \right\} \stackrel{!}{=} 1. \quad (39)$$

Turning our attention to the non-valence region, for $x < \zeta$ we find for the p^- integral in Eq. (35):

$$\mathcal{H}(x, \zeta, t) \Big|_{x<\zeta} = \frac{N_c N_f g^2 C^2}{2} \int \frac{d^2 p^\perp}{(2\pi)^3} \left\{ \frac{1}{p^{\perp 2} + m^2 - \bar{x}M^2} + \frac{2x/\zeta - 1}{(p^\perp + d^\perp)^2 + m^2 + x(x-\zeta)t/\zeta^2} \right. \\ \left. + \frac{y[(2x-\zeta)M^2 + (1-x)t]}{[p^{\perp 2} + m^2 - \bar{x}M^2][(p^\perp + d^\perp)^2 + m^2 + x(x-\zeta)t/\zeta^2]} \right\}, \quad (40)$$

where now $y = x/\zeta$. The remaining integrals may again be evaluated analytically and we get the analogous result as the one for $x > \zeta$, Eq. (37),

$$\mathcal{H}(x, \zeta, t) \Big|_{x < \zeta} = \frac{N_c N_f g^2 C^2}{2} \frac{1}{(2\pi)^2} \sum_{j=0}^2 c_j \left\{ -\log \frac{m_j^2}{m^2} - \frac{1}{2} \log \frac{m_j^2 - \bar{x} M^2}{m_j^2} - \frac{2x/\zeta - 1}{2} \log \frac{m_j^2 - \bar{y} t}{m_j^2} + \frac{(2x - \zeta) M^2 + (1 - x) t}{2} \tilde{M}(m_j, \Delta, P) \right\}. \quad (41)$$

A few properties of the final result may immediately be recognized. First, the total GPD is again continuous at $x = \zeta$, even though the derivative at this point is not. Second, the sum rule of Eq. (3) is identically fulfilled. Third, as noted above, $\mathcal{H}(1, \zeta, t) \neq 0$, but from Eq. (40) we see that $\mathcal{H}(0, \zeta, t) = 0$ for $\zeta \neq 0$.

Note that at $x = 1$, the GPD becomes independent of t and ζ , it only depends on the bound state mass M via the normalization constant $g^2 C^2$. In particular, in the chiral limit, when $M^2 = 0$, the value of $\mathcal{F}(x, \zeta, t)$ at $x = 1$ is simply given by

$$\mathcal{H}(1, \zeta, t) = 1. \quad (42)$$

In spite of these peculiarities, we note again that Eq. (3) is always exactly satisfied, as we checked numerically. In addition, the polynomiality condition takes a very simple form in the chiral limit. When $M^2 = 0$, the following relation may be shown to hold:

$$\int_0^1 x^{N-1} \mathcal{H}(x, \zeta, 0) dx = \frac{1}{N} \left(1 - \frac{\zeta^N}{N+1} \right), \quad (43)$$

i.e., at zero momentum transfer, the polynomiality condition is fulfilled. Again, for $N = 1$, Eq. (43) reproduces Eq. (3) in the case $t = 0$. In Table I we give a comparison of moments of GPDs in the scalar model, the NJL model and

TABLE I: The moments of the GPDs, as defined by Eq. (17), for the pion in various models. SED and NJL give the analytic results in the chiral limit, $M = 0$, for the scalar model, Eq. (18), and the model of Nambu – Jona-Lasinio, Eq. (43), respectively. $F_N^v = F_N(\zeta = 0, t = 0)$ and $F_N^{nv} = F_N(\zeta = 1, t = 0)$ represent pure valence and pure non-valence contributions, respectively.

Model	$F_2^v [F_2^{nv}]$	$F_3^v [F_3^{nv}]$	$F_4^v [F_4^{nv}]$	$F_5^v [F_5^{nv}]$	$F_6^v [F_6^{nv}]$	$F_7^v [F_7^{nv}]$
ref. [27] ^a	0.503 [0.312]	0.312 [0.217]	0.215 [0.161]	0.16 [0.125]	0.123 [0.101]	0.098 [0.083]
ref. [7]		0.25 [—]				
ref. [33]		0.29 [—]				
SED	$\frac{1}{2} [\frac{1}{2}]$	$\frac{3}{10} [\frac{9}{20}]$	$\frac{1}{5} [\frac{2}{5}]$	$\frac{1}{7} [\frac{5}{14}]$	$\frac{3}{28} [\frac{9}{28}]$	$\frac{1}{12} [\frac{7}{24}]$
NJL	$\frac{1}{2} [\frac{1}{3}]$	$\frac{1}{3} [\frac{1}{4}]$	$\frac{1}{4} [\frac{1}{5}]$	$\frac{1}{5} [\frac{1}{6}]$	$\frac{1}{6} [\frac{1}{7}]$	$\frac{1}{7} [\frac{1}{8}]$

^aThe results for F_N^{nv} of this reference have been divided by a factor 2, in order to comply with a different definition of variables.

results of other works. We see a rather nice agreement of the NJL results with those of ref. [27], especially for low moments, while for larger N , our results tend to be somewhat larger. The most striking difference appears for the non-valence contributions in the scalar model, which are about a factor of 2 larger than in the NJL model (note that for $t = 0$, the skewedness parameter ζ is actually confined to be zero, see the remark after Eq. (5), but like in ref. [27], we use our analytical formulas, Eqs. (18,43), to continue the results to $\zeta = 1$). Another interesting feature evidenced by the results in this table is the apparent identity

$$F_N^{nv} = F_{N+1}^v, \quad (44)$$

which is analytically fulfilled in the NJL model, see Eq. (43), but also seems to hold for the numerical results of ref. [27]. Only in the scalar model this relation does not hold due to the larger values of the non-valence contributions mentioned above.

Finally we note that in the chiral limit, $M^2 = 0$ and at zero momentum transfer, $t = 0$, we reproduce the analytic results of ref. [7], namely:

$$\mathcal{H}(x, \zeta, 0) = \frac{x}{\zeta} \theta(\zeta - x) + \theta(x - \zeta), \quad (45)$$

so in particular, $\mathcal{H}(x, 1, 0) = x$ and $\mathcal{H}(x, 0, 0) = 1$. This form may be compared with the corresponding result in the scalar model, see Eq. (20). Eq. (45) also implies that in the chiral limit we get a quark distribution function that is equal to unity. This coincides with the results obtained in refs. [30, 31, 32].

In Fig. 4 we give some examples of GPDs in the NJL model. They illustrate two distinct behaviors characterized by the strength of the binding, i.e., the weak and strong binding limits. For zero binding, there is no spontaneous symmetry breaking, thus no pion and the constituents are free. For weak binding, we expect therefore a very similar behavior of the GPDs to the one discussed in scalar electrodynamics. This similarity can be seen by comparing the corresponding graphs of Figs. 2 and 4. In the weak binding limit we note again the appearance of two peaks at $x = 1/2$ and $x = (1 + \zeta)/2$, which go over into δ -functions in the exact limit $M^2 = 4m^2$, just as in the scalar case, see Eq. (19), only the form factor $F(t)$ will differ from one model to the other.

As soon as there is binding, chiral symmetry is spontaneously broken, and the GPDs differ more and more from the free ones as we approach the $M = 0$ limit with massive constituent quarks. The most striking feature evidenced by these figures is the non-vanishing of the distribution functions at the boundary, $x = 1$, and (for $\zeta = 0$) $x = 0$. As mentioned above, the value at $x = 1$ is independent of Q^2 and ζ , it only depends on the binding energy, varying from zero, in the free case, to unity in the deep binding limit of zero pion mass. This effect is associated with the breaking of chiral symmetry, as we shall discuss in more detail later on. The value for $x = 0$, $\zeta = 0$, does depend on Q^2 (decreasing like $1/Q^2$ for large Q^2), but for fixed Q^2 , it depends on the binding energy in the same way as the value at $x = 1$, vanishing again only in the zero-binding limit. Furthermore, the distribution functions become relatively more concentrated around $x = 1$ for large Q^2 , which is just a consequence of the constant value of the distribution function at $x = 1$.

Note also that for large $Q^2 = -t$, the distribution functions become negative in the central region. This can not be seen from the graphs displayed in Fig. 4, but it is a consequence of the relative sign between the terms of the coefficient of the last logarithm in Eq. (37).

B. Electromagnetic form factor

In order to understand better the above results, we may want to calculate the electromagnetic form factor in the NJL model which is given by the x -integrated parton distribution, see Eq. (3). This has been done already in several works [25, 34, 35], but we want to investigate the relation with the present results. Calculating again the current in impulse approximation, (the second diagram of Fig. 1 vanishes again as in the scalar case, even though it would contribute to the GPDs), we find:

$$(P + P')^\mu F(Q^2) = 4iN_c N_f g^2 C^2 \int \frac{d^4 p}{(2\pi)^4} \frac{(p^\mu + P^\mu + \Delta^\mu)(p^2 - m^2) + p \cdot \Delta P^\mu - P \cdot \Delta p^\mu - (2p^\mu + \Delta^\mu) p \cdot P}{(p^2 - m^2)[(p + \Delta)^2 - m^2][(P - p)^2 - m^2]}. \quad (46)$$

Rewriting the denominator under the integral as

$$(p^\mu + P^\mu + \Delta^\mu)(p^2 - m^2) + p \cdot \Delta P^\mu - P \cdot \Delta p^\mu - (2p^\mu + \Delta^\mu) p \cdot P = [(P - p)^2 - m^2 - M^2 - Q^2/2] p^\mu + [p^2 - m^2 + (p + \Delta)^2 - m^2 + Q^2] \frac{P^\mu}{2} + [p^2 - m^2 + (P - p)^2 - m^2 - M^2] \frac{\Delta^\mu}{2},$$

and using some relations of appendix B, we arrive at

$$F(Q^2) = iN_c N_f g^2 C^2 \frac{(Q^2/2 + M^2)I(\Delta) + M^2 I(P) - M^4 M(\Delta, -P)}{Q^2/4 + M^2}. \quad (47)$$

We checked numerically (by applying the same Pauli-Villars regularization method) that this form factor is exactly reproduced by integrating our result for the GPD over x . This means that the non-vanishing distribution functions (at $x = 1$) are implicitly present in the result of Eq. (47). Note that in the chiral limit, $M^2 = 0$, we simply have

$$F(Q^2) = 2iN_c N_f g^2 C^2 I(\Delta) = 1 - R(Q^2)/I(0), \quad (48)$$

where for small Q^2 , $R(Q^2)$ is given by

$$R(Q^2) = \frac{i}{16\pi^2} \frac{Q^2}{6m^2}, \quad (49)$$

so together with the relation $f_\pi^2 = -12im^2 I(0)$, we can evaluate the root-mean squared radius of the pion in this model via $\langle r_\pi \rangle^2 = -6 \partial F(Q^2)/\partial Q^2 = 3f_\pi^{-2}/(4\pi^2)$, which is the same as in ref. [25]. With $f_\pi = 93$ MeV, we find the numerical value of $\langle r_\pi \rangle^2 = (0.585 \text{ fm})^2$, to be compared to the experimental value of $(0.66 \text{ fm})^2$. Note, however, that Eq. (49) is valid only in the limit when the cut-off goes to infinity, for the finite cut-off as specified in appendix A, the root mean squared radius gets multiplied by a factor ~ 0.89 .

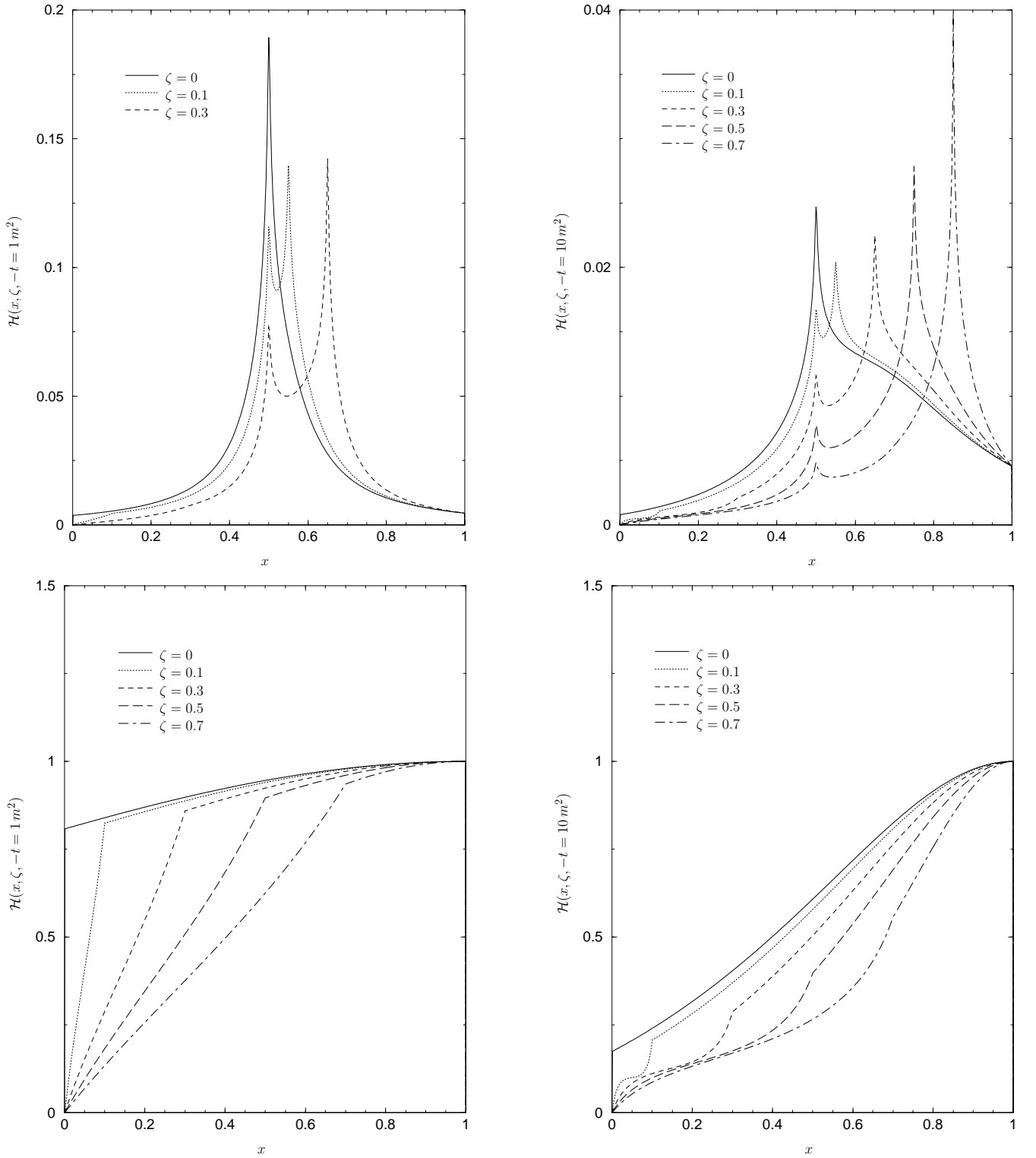


FIG. 4: Generalized parton distributions in the Nambu – Jona-Lasinio model for different values of the bound state mass M and momentum transfers t . The top row gives results for $M/m = 2 - (1/137)^2/4$, while on the bottom $M = 0$ MeV. The graphs in the left column are for a momentum transfer $-t = 1 m^2$, and on the right, $-t = 10 m^2$. Note that the sum rule of Eq. (3) is exactly satisfied for each graph.

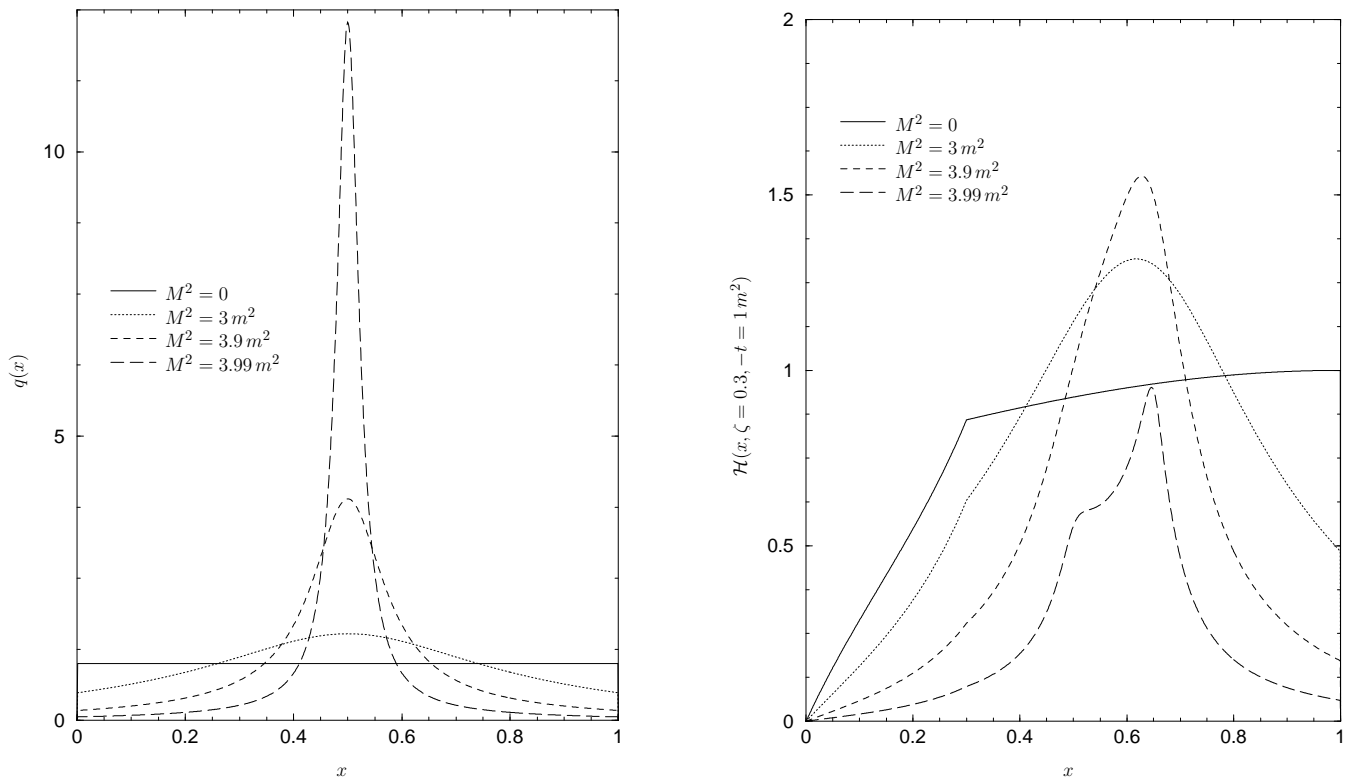


FIG. 5: Generalized parton distribution functions in the Nambu – Jona-Lasinio model as functions of x for different bound state masses M . On the left figure we have the quark distribution function $q(x) = \mathcal{H}(x, 0, 0)$, on the right we have $\mathcal{H}(x, \zeta = 0.3, -t = 1 m^2)$. The constituent mass is kept fixed at $m = 241$ MeV.

V. DISCUSSION

The results obtained in the scalar electrodynamics model show a perfect realization of all wishful ingredients. The calculation is exact, finite and satisfies all the desired properties, i.e., the GPDs have the correct support and vanish at the boundary regions, while the sum rule and the polynomiality condition are exactly verified. From the physical point of view, the GPDs show a realization in terms of quasi-free constituents in the weak binding limit. As the binding increases one is confronted with the dynamics as derivable from a non trivial momentum distribution determined by the corresponding Bethe-Salpeter wave function, a feature also appearing in other model calculations [14]. The physical effect associated with t and ζ is naturally represented in the GPDs. The variable t tends to push the constituent distribution towards higher values of x , which corresponds to an input of momentum transfer into the system, while the variable ζ incorporates the description of virtual pairs. Unfortunately this model is not very realistic for the pion (perhaps it might be better fit for a description of the nucleon) and our results represent only qualitative features of how the dynamics might influence the distributions.

For the NJL model the calculation requires regularization. The latter certainly influences the results, as has been discussed in ref. [29], where the Pauli-Villars method was compared to the one of Brodsky-Lepage with different results. The Pauli-Villars method seems to be the only one compatible with all the symmetry requirements [31], which is the reason for our choice. A caveat that should be emphasized is that the model does not only contain the dynamics expressed in the Lagrangian, but also the one derived from the regularization procedure.

The NJL calculation retains some nice properties, in particular it preserves the sum rule and the polynomiality condition. Physically it is also very appealing since we can distinguish features associated with the weak and strong coupling regimes. In Fig. 5 we show on the left hand side the variation of the quark distribution function with the binding energy. As the binding energy increases we change softly from a delta type behavior, at zero binding, to a constant behavior in the strong binding regime. This figure also illustrates nicely the phase transition associated with the spontaneous breaking of chiral symmetry. Suppose we keep the mass of the bound state fixed at $M^2 = 0$ and consider the variation of $q(x)$ with m . It is clear that we will always have $q(x) = 1$ for any value of m , except when $m = 0$, where the distribution function changes discontinuously to $q(x) = \delta(x - 1/2)$. The effect of t and ζ described

for scalar electrodynamics persist, as can be seen in the graph on the right hand side of this figure, i.e., t pushes the distribution to higher values of x and ζ introduces virtual pairs into the description of the system.

The problem we face is the non-vanishing of the GPDs at the boundary, i.e., $\mathcal{H}(x, \zeta, t) \neq 0$ for $x = 1$ and (if $\zeta = 0$) $x = 0$. For the structure function $q(x) = \mathcal{H}(x, 0, 0)$, this feature was already noted in refs. [30, 31, 32] and it is obviously present in an implicit way in the results of electromagnetic form factor calculations [25, 34, 35]. Curiously, we did not find a discussion of this peculiarity, with respect to its physical interpretation, in any of these references. To elucidate the matter, one might investigate the mass dependence of the GPDs at a given point x . In our calculation we get for $x = 1$ the general expression

$$\mathcal{H}(x = 1, \zeta, t) = \frac{F_0}{F_0 - 1 + \left(\sqrt{\frac{4m^2}{M^2} - 1} + \frac{1}{\sqrt{\frac{4m^2}{M^2} - 1}} \right) \arctan \left(\frac{1}{\sqrt{\frac{4m^2}{M^2} - 1}} \right) + \dots}, \quad (50)$$

where $F_0 = 16i\pi^2 I(0)$, with $I(p)$ given by Eq. (B6), is a regularization constant and the dots denote terms of higher order in M^2/Λ^2 , where Λ is the cut-off parameter in the Pauli-Villars regularization, see Appendix A. This equation illustrates the dependence on the bound state mass, and also the regularization scheme dependence is apparent. It is clear from Eq. (50) that $\mathcal{H}(x = 1, \zeta, t)$ vanishes for zero binding ($M^2 = 4m^2$) while it is non-vanishing for $M^2 < 4m^2$. As soon as the interaction binds the quarks into a pion, $M^2 < 4m^2$ and at the same time, chiral symmetry is spontaneously broken. Therefore, our previous observation, that the non-zero value at $x = 1$ is related to chiral symmetry breaking, is justified. Moreover in the NJL model we recover the result that in the chiral limit, $M^2 = 0$, $q(x)$ is independent of x and equal to unity. It must be recalled that this feature also arises in the 't Hooft model [36], where one finds $q(x) = \text{const.}$ for zero-mass pions.

It has to be stressed that the feature of a non-vanishing distribution function at the end-points in our model has nothing to do with what is usually called the support problem. The latter is characterized by a non-vanishing distribution function outside the physical region, i.e. $\mathcal{H}(x, \zeta, t) \neq 0$ for $x < \zeta - 1$ or $x > 1$, while in our calculations, the GPDs explicitly vanish there. It is therefore really a discontinuity that we encounter at the physical boundary.

The physical interpretation of this feature is not clear. The $x = 1$ region corresponds to elastic scattering of the photon from the bound system, thus the distributions for the constituents should vanish at this point. That they do not in the NJL model could be an artifact of the regularization but since it also occurs in the 't Hooft model one may be inclined to think that there is a deeper physical reason for it. Moreover, it showed up already in several model calculations. In refs. [7, 37], a momentum dependent constituent quark mass (or equivalently, a constituent quark form factor) was introduced to force the distribution functions to be zero at the end points, while in ref. [38] the problem was resolved by applying the QCD evolution equations [39]. The evolution of our GPDs to higher renormalization points is currently considered. On the other hand, the conceptual problem encountered here is only apparent if one relies on the interpretation of quark structure functions as probability distributions. It has been shown recently [40] that this is not necessarily correct because final state interactions between the scattered and the spectator particle affect the structure functions profoundly. The fact that the distributions do not vanish at $x = 0$ for $\zeta = 0$ is just a consequence of the non-vanishing at $x = 1$ and does not seem to introduce any new conceptual problem.

VI. CONCLUSION

In this work, we presented a benchmark calculation of generalized parton distribution functions using a covariant Bethe-Salpeter approach in scalar electrodynamics and in the Nambu – Jona-Lasinio model. No assumptions have gone into the determination of wave functions or any other ingredient of the calculation. The only approximations employed are the ladder approximation for the determination of the Bethe - Salpeter bound state amplitude (which is, of course, still a fully covariant object in this case), and in the determination of the current matrix elements, we have restricted ourselves to the impulse approximation. As a result, no important features required by general physical considerations, like symmetry properties, sum rules, etc., have been violated and we recover them in our numerical results. For the scalar model, the calculation evidences all desirable features and we basically recover results obtained in similar studies. In the NJL model, we found that the GPDs do not vanish at the boundary of the kinematic region, i.e., at $x = 0$ and $x = 1$, a feature which seems to be associated with spontaneous chiral symmetry breaking.

Before finishing we must recall that our calculation is valid at the hadronic scale, i.e., at a low momentum renormalization point. Evolution to higher momenta is necessary to describe deep inelastic scattering data. It will be interesting to see how the described features of the NJL model will change under evolution.

Acknowledgments

This work was supported by the European Commission IHP program under contract HPRN-CT-2000-00130, MCYT (Spain) under contracts BFM2001-3563-C02-01 and BMF2001-0262, and Generalitat Valenciana under contract GV01-216. One of us (V.V.) would like to thank the Physics Department of Seoul National University, and Prof. Dong-Pil Min in particular, for the hospitality extended to him during the last stages of this work.

APPENDIX A: REGULARIZATION

We shall use the Pauli-Villars regularization in order to render the occurring integrals finite. This means that for the integrals defined by Eqs. (B1-B3), we make the replacement

$$\int \frac{d^4 p}{(2\pi)^4} f(p; m^2) \longrightarrow \int \frac{d^4 p}{(2\pi)^4} \sum_{j=0}^2 c_j f(p; m_j^2), \quad (\text{A1})$$

with $m_j^2 = m^2 + j\Lambda^2$, $c_0 = -c_1/2 = c_2 = 1$. Following ref. [25] we determine the regularization parameters Λ and m by calculating the pion decay constant and the quark condensate (in the chiral limit) via

$$f_\pi^2 = -\frac{3m^2}{4\pi^2} \sum_{j=0}^2 c_j \log(m_j^2/m^2), \quad \langle \bar{u}u \rangle = -\frac{3m}{4\pi^2} \sum_{j=0}^2 c_j m_j^2 \log(m_j^2/m^2). \quad (\text{A2})$$

With the conventional values $\langle \bar{u}u \rangle = -(250 \text{ MeV})^3$ and $f_\pi = 93 \text{ MeV}$, we get $m = 241 \text{ MeV}$ and $\Lambda = 859 \text{ MeV}$.

APPENDIX B: ELEMENTARY INTEGRALS

$$I_1 \equiv \int \frac{d^4 k}{(2\pi)^4} \frac{1}{k^2 - m^2 + i\epsilon}, \quad (\text{B1})$$

$$I(p) \equiv \int \frac{d^4 k}{(2\pi)^4} \frac{1}{(k^2 - m^2 + i\epsilon)((k+p)^2 - m^2 + i\epsilon)}, \quad (\text{B2})$$

$$M(p_1, p_2) \equiv \int \frac{d^4 k}{(2\pi)^4} \frac{1}{(k^2 - m^2 + i\epsilon)(k_1^2 - m^2 + i\epsilon)(k_2^2 - m^2 + i\epsilon)}, \quad (\text{B3})$$

with $k_i = k + p_i$. From these definitions the following relation may be deduced:

$$\int \frac{d^4 k}{(2\pi)^4} \frac{k^\mu}{(k^2 - m^2 + i\epsilon)((k+p)^2 - m^2 + i\epsilon)} = -\frac{1}{2} p^\mu I(p). \quad (\text{B4})$$

With the Pauli-Villars regularization of Eq. (A1) we have the following simple expressions:

$$I_1 = -\frac{i}{16\pi^2} \sum_{j=0}^2 c_j m_j^2 \log(m_j^2/m^2), \quad (\text{B5})$$

$$I(p) = -\frac{i}{16\pi^2} \sum_{j=0}^2 c_j \left\{ \log(m_j^2/m^2) + \sqrt{\frac{p^2 - 4m_j^2}{p^2}} \log \frac{1 - \sqrt{\frac{p^2 - 4m_j^2}{p^2}}}{1 + \sqrt{\frac{p^2 - 4m_j^2}{p^2}}} \right\}, \quad (\text{B6})$$

$$\tilde{I}(P) \equiv \int \frac{d^4 k}{(2\pi)^4} \frac{\delta(x - k^+/P^+)}{(k^2 - m^2 + i\epsilon)((k-P)^2 - m^2 + i\epsilon)} = \frac{i}{16\pi^2} \sum_{j=0}^2 c_j \log \frac{m_j^2 - \bar{x}P^2}{m^2}, \quad (\text{B7})$$

$$\begin{aligned}
\tilde{M}(m, \Delta, P) &\equiv -16i\pi^2 \int \frac{d^4 k}{(2\pi)^4} \frac{\delta(x - k^+/P^+)}{(k^2 - m^2 + i\epsilon)((k + \Delta)^2 - m^2 + i\epsilon)((P - k)^2 - m^2 + i\epsilon)} = \\
&= \begin{cases} \frac{y}{\sqrt{D}} \log \frac{d^{\perp 2} + 2m^2 - (\bar{x}M^2 + \bar{y}t) + \sqrt{D}}{d^{\perp 2} + 2m^2 - (\bar{x}M^2 + \bar{y}t) - \sqrt{D}}, & \left| \begin{array}{l} y = \frac{x}{\zeta}, \quad d^\perp = y(\zeta P^\perp + \Delta^\perp) \\ D = [d^{\perp 2} - (\bar{x}M^2 + \bar{y}t)]^2 - 4\bar{x}\bar{y}M^2 t + 4d^{\perp 2} m^2 \end{array} \right|, & 0 < x < \zeta, \\ \frac{y}{\sqrt{D}} \log \frac{d^{\perp 2} + 2m^2 - (\bar{x} + \bar{y})M^2 + \sqrt{D}}{d^{\perp 2} + 2m^2 - (\bar{x} + \bar{y})M^2 - \sqrt{D}}, & \left| \begin{array}{l} y = \frac{1-x}{1-\zeta}, \quad d^\perp = y(\zeta P^\perp + \Delta^\perp) \\ D = [d^{\perp 2} - (\bar{x} + \bar{y})M^2]^2 - 4\bar{x}\bar{y}M^4 + 4d^{\perp 2} m^2 \end{array} \right|, & \zeta < x < 1, \\ 0 & & \text{otherwise.} \end{cases} \quad (\text{B8})
\end{aligned}$$

In the last integral, $\zeta = -\Delta^+/P^+$ and $\bar{x} = x(1-x)$, $\bar{y} = y(1-y)$ in each case. Furthermore, $M^2 = P^2$, $t = \Delta^2$, and no Pauli-Villars regularization was employed since the integral is convergent.

APPENDIX C: OTHER CONVENTIONS

A different convention than the one we used in this paper, which emphasizes the symmetry between the incoming and outgoing hadron momenta, consists in defining the variables x and ζ using average momenta:

$$X = \frac{\bar{p}^+}{\bar{P}^+}, \quad \xi = -\frac{\Delta^+}{2\bar{P}^+}, \quad (\text{C1})$$

where $\bar{P} = (P + P')/2 = P + \Delta/2$ and $\bar{p} = (p + p')/2 = p + \Delta/2$. These variables are related to our previously defined ones, Eq. (4), by

$$x = \frac{X + \xi}{1 + \xi}, \quad \zeta = \frac{2\xi}{1 + \xi}, \quad X = \frac{2x - \zeta}{2 - \zeta}, \quad \xi = \frac{\zeta}{2 - \zeta}. \quad (\text{C2})$$

With this definitions, the sum rule of Eq. (3) is simply written as

$$\int \mathcal{H}(X, \xi, t) dX = F(t). \quad (\text{C3})$$

-
- [1] D. Müller, D. Robaschik, B. Geyer, F. M. Dittes and J. Horejsi: *Wave functions, evolution equations and evolution kernels from light-ray operators of QCD*, Fortschr. Phys. **42** (1994) 101, ([hep-ph/9812448](#)).
 - [2] X.-D. Ji: *Deeply-virtual compton scattering*, Phys. Rev. **D55** (1997) 7114–7125, ([hep-ph/9609381](#)).
 - [3] A. V. Radyushkin: *Nonforward parton distributions*, Phys. Rev. **D56** (1997) 5524–5557, ([hep-ph/9704207](#)).
 - [4] X.-D. Ji: *Off-forward parton distributions*, J. Phys. **G24** (1998) 1181–1205, ([hep-ph/9807358](#)).
 - [5] M. Diehl, T. Feldmann, R. Jakob and P. Kroll: *Linking parton distributions to form factors and compton scattering*, Eur. Phys. J. **C8** (1999) 409–434, ([hep-ph/9811253](#)).
 - [6] M. Diehl, T. Feldmann, R. Jakob and P. Kroll: *The overlap representation of skewed quark and gluon distributions*, Nucl. Phys. **B596** (2001) 33–65, ([hep-ph/0009255](#)).
 - [7] M. V. Polyakov and C. Weiss: *Skewed and double distributions in pion and nucleon*, Phys. Rev. **D60** (1999) 114017, ([hep-ph/9902451](#)).
 - [8] M. Diehl, T. Feldmann, P. Kroll and C. Vogt: *The perturbative limit of the two-pion light-cone distribution amplitude*, Phys. Rev. **D61** (2000) 074029, ([hep-ph/9912364](#)).
 - [9] X.-D. Ji, W. Melnitchouk and X. Song: *A study of off-forward parton distributions*, Phys. Rev. **D56** (1997) 5511–5523, ([hep-ph/9702379](#)).
 - [10] I. V. Anikin, D. Binosi, R. Medrano, S. Noguera and V. Vento: *Single spin asymmetry parameter from deeply virtual Compton scattering of hadrons up to twist-3 accuracy. I: Pion case*, Eur. Phys. J. **A14** (2002) 95–103, ([hep-ph/0109139](#)).
 - [11] V. Y. Petrov et al.: *Off-forward quark distributions of the nucleon in the large- N_c limit*, Phys. Rev. **D57** (1998) 4325–4333, ([hep-ph/9710270](#)).
 - [12] M. Penttinen, M. V. Polyakov and K. Goeke: *Helicity skewed quark distributions of the nucleon and chiral symmetry*, Phys. Rev. **D62** (2000) 014024, ([hep-ph/9909489](#)).
 - [13] S. Scopetta and V. Vento: *Generalized parton distributions and constituent quarks*, [hep-ph/0207218](#).
 - [14] S. Scopetta and V. Vento: *Generalized parton distributions in constituent quark models*, [hep-ph/0201265](#).
 - [15] K. J. Golec-Biernat and A. D. Martin: *Off-diagonal parton distributions and their evolution*, Phys. Rev. **D59** (1999) 014029, ([hep-ph/9807497](#)).

- [16] P. A. M. Guichon and M. Vanderhaeghen: *Virtual Compton scattering off the nucleon*, Prog. Part. Nucl. Phys. **41** (1998) 125–190, (hep-ph/9806305).
- [17] B. Desplanques, L. Theußl and S. Noguera: *Effective boost and 'point-form' approach*, Phys. Rev. **C65** (2002) 038202, (nucl-th/0107029).
- [18] A. Amghar, B. Desplanques and L. Theußl: *Comparison of form factors calculated with different expressions for the boost transformation*, nucl-th/0202046.
- [19] B. C. Tiburzi and G. A. Miller: *Exploring skewed parton distributions with two body models on the light front. I: Bimodality*, Phys. Rev. **C64** (2001) 065204, (hep-ph/0104198).
- [20] B. C. Tiburzi and G. A. Miller: *Exploring skewed parton distributions with two-body models on the light front. II: Covariant Bethe-Salpeter approach*, Phys. Rev. **D65** (2002) 074009, (hep-ph/0109174).
- [21] S. J. Brodsky, M. Diehl and D. S. Hwang: *Light-cone wavefunction representation of deeply virtual Compton scattering*, Nucl. Phys. **B596** (2001) 99–124, (hep-ph/0009254).
- [22] Y. Nambu and G. Jona-Lasinio: *Dynamical model of elementary particles based on an analogy with superconductivity. I*, Phys. Rev. **122** (1961) 345–358.
- [23] Y. Nambu and G. Jona-Lasinio: *Dynamical model of elementary particles based on an analogy with superconductivity. II*, Phys. Rev. **124** (1961) 246–254.
- [24] U. Vogl and W. Weise: *The Nambu and Jona Lasinio model: Its implications for hadrons and nuclei*, Prog. Part. Nucl. Phys. **27** (1991) 195–272.
- [25] S. P. Klevansky: *The Nambu-Jona-Lasinio model of quantum chromodynamics*, Rev. Mod. Phys. **64** (1992) 649–708.
- [26] C. Vogt: *Skewed quark distribution of the pion at large momentum transfer*, Phys. Rev. **D64** (2001) 057501, (hep-ph/0101059).
- [27] H.-M. Choi, C.-R. Ji and L. S. Kisslinger: *Skewed quark distribution of the pion in the light-front quark model*, Phys. Rev. **D64** (2001) 093006, (hep-ph/0104117).
- [28] L. S. Kisslinger, H.-M. Choi and C.-R. Ji: *Pion form factor and quark mass evolution in a light-front Bethe-Salpeter model*, Phys. Rev. **D63** (2001) 113005, (hep-ph/0101053).
- [29] R. M. Davidson and E. Ruiz Arriola: *Parton distributions functions of pion, kaon and eta pseudoscalar mesons in the NJL model*, hep-ph/0110291.
- [30] R. M. Davidson and E. Ruiz Arriola: *Structure functions of pseudoscalar mesons in the SU(3) NJL model*, Phys. Lett. **B348** (1995) 163–169.
- [31] H. Weigel, E. Ruiz Arriola and L. P. Gamberg: *Hadron structure functions in a chiral quark model: Regularization, scaling and sum rules*, Nucl. Phys. **B560** (1999) 383–427, (hep-ph/9905329).
- [32] T. Shigetani, K. Suzuki and H. Toki: *Pion structure function in the Nambu and Jona-Lasinio model*, Phys. Lett. **B308** (1993) 383–388, (hep-ph/9402286).
- [33] A. V. Belitsky: *Quark distribution in the pion from QCD sum rules with nonlocal condensates*, Phys. Lett. **B386** (1996) 359–369, (hep-ph/9604329).
- [34] V. Bernard and U. G. Meissner: *Electromagnetic structure of the pion and the kaon*, Phys. Rev. Lett. **61** (1988) 2296.
- [35] H. J. Schulze: *The pion form-factor at zero and finite temperature in the Nambu-Jona-Lasinio model*, J. Phys. **G20** (1994) 531–548.
- [36] G. 't Hooft: *A two-dimensional model for mesons*, Nucl. Phys. **B75** (1974) 461.
- [37] M. Praszalowicz and A. Rostworowski: *Pion generalized parton distributions in the non-local NJL model*, hep-ph/0205177.
- [38] E. R. Arriola and W. Broniowski: *Pion light-cone wave function and pion distribution amplitude in the Nambu-Jona-Lasinio model*, hep-ph/0207266.
- [39] D. Müller: *The evolution of the pion distribution amplitude in next- to-leading-order*, Phys. Rev. **D51** (1995) 3855–3864, (hep-ph/9411338).
- [40] S. J. Brodsky, P. Hoyer, N. Marchal, S. Peigné and F. Sannino: *Structure functions are not parton probabilities*, Phys. Rev. **D65** (2002) 114025, (hep-ph/0104291).